

# Magnetic trapping and Zeeman relaxation of imidogen ( $\text{NH } X^3\Sigma^-$ )

Wesley C. Campbell,<sup>1,2,\*</sup> Edem Tsikata,<sup>1,2</sup> Laurens van Buuren,<sup>1,2,†</sup> Hsin-I Lu,<sup>3,2</sup> and John M. Doyle<sup>2,1</sup>

<sup>1</sup>*Department of Physics, Harvard University,  
Cambridge, Massachusetts 02138, USA*

<sup>2</sup>*Harvard-MIT Center for Ultracold Atoms,  
Cambridge, Massachusetts 02138, USA*

<sup>3</sup>*Division of Engineering and Applied Sciences,  
Harvard University, Cambridge, MA 02138, USA*

(Dated: July 17, 2018)

## Abstract

Imidogen (NH) radicals are magnetically trapped and their Zeeman relaxation and energy transport collision cross sections with helium are measured. Continuous buffer-gas loading of the trap is direct from a room-temperature molecular beam. The Zeeman relaxation (inelastic) cross section of magnetically trapped electronic, vibrational and rotational ground state imidogen in collisions with  $^3\text{He}$  is measured to be  $3.8 \pm 1.1 \times 10^{-19} \text{ cm}^2$  at 710 mK. The NH-He energy transport cross section is also measured, indicating a ratio of diffusive to inelastic cross sections of  $\gamma = 7 \times 10^4$ , in agreement with recent theory [1].

Driven by the promise of new physics and applications, the field of cold molecular physics has undergone tremendous growth in the past decade [2, 3]. In particular, polar molecules have been proposed [4, 5] as qubits for quantum information processing and for studies of highly correlated condensed matter systems [6]. Cold molecules are also very promising candidates for fundamental physics measurements, such as the search for the electric dipole moment of the electron [7] and time variation of the electron-proton mass ratio [8]. Chemistry with cold molecules may be possible to observe in a new quantum regime where the large deBroglie wavelength and long interaction times of reactants can reopen chemical reaction pathways through tunneling [9, 10]. A key to realizing these new phenomena is the production of cold, trapped, high-density samples of polar molecules.

The complexity inherent in molecules, compared to atoms, makes working with them difficult; the rich internal structure of molecules opens decay modes that, for example, could make evaporative cooling difficult to achieve [11]. Preparation of cold, dense samples of trapped molecules should provide a pathway to measure cold molecule collisions, critical to elucidating the suitability of molecules for evaporative [12, 13, 14] and sympathetic cooling [15]. So far, several methods have been used to create (ultra-)cold molecules. Production of ultracold molecules from ultracold atoms has been realized through photo and Feshbach association [16, 17]. Direct cooling or slowing of initially hot polar molecules has also been demonstrated using Stark deceleration [3, 18], optical slowing [19], billiard-like collisions [20], and buffer-gas cooling [21]. Buffer gas cooling uses cryogenic helium gas to cool hot molecules (or atoms). When done in the presence of a magnetic trapping field this can cause the molecules to fall into the conservative trap potential. The first successful trapping of polar molecules was accomplished in our group with buffer-gas loading of CaH, and we know of several other laboratories using buffer-gas loading of magnetic traps [22, 23, 24]. Other molecules (VO [25], CaF [26] and CrH [27]) have also been studied with buffer-gas loading but in all those cases there were loss mechanisms that prevented trapping for extended periods of time.

Despite great progress in the field of cold molecules, no technique has yet realized trapped densities sufficiently high to observe polar molecule-molecule collisions. However, the buffer gas method allowed studies of cold atom-polar molecule spin relaxation of trapped molecules (He-CaH and CaF [21, 26]). These measurements in combination with theory began to uncover the fundamental processes of cold molecule collisions in traps. CaH has a  $^2\Sigma$  ground

state, perhaps the simplest type of magnetically trappable molecule. Although this provided important information on the nature of cold molecule collisions, it was incomplete as there are a variety of molecules. For example,  $^3\Sigma$  molecules carry with them new internal dynamics, such as the spin-spin interaction, which allows for direct coupling of the rotation during a collision (unlike the  $^2\Sigma$  case) [28]. The current vigorous pursuit of high density samples of cold molecules has led several groups to the imidogen (NH) radical. Cold, trapped imidogen is being studied theoretically [1, 14, 15, 29] and pursued experimentally [30, 31, 32], and a scheme for continuous loading of imidogen into a magnetic trap has been proposed for Stark deceleration [33].

In this Letter, we demonstrate magnetic trapping of ground state ( $X^3\Sigma^-$ ) imidogen radicals and make a direct measurement of the spin relaxation rate in collisions with  $^3\text{He}$ . Imidogen is continuously loaded directly from a room-temperature molecular beam into a magnetic trap *via* buffer-gas cooling. More than  $10^8$  molecules are loaded into the trap and are observed for longer than 1 s, with  $1/e$  lifetimes exceeding 200 ms. The energy transport collision rate is also measured, allowing the determination of the ratio of the diffusive to inelastic cross sections in this system, found to be  $\gamma = \sigma_d/\sigma_{\text{in}} = 7 \times 10^4$ .

We chose to study imidogen (NH) due to its internal structure, predicted collisional properties, and for technical reasons. The  $X^3\Sigma^-$  ground state has a  $2\mu_B$  magnetic moment and 1.38 Debye electric dipole moment. The imidogen radicals can be produced in an ammonia discharge [34] and detected in absorption or fluorescence on the  $A^3\Pi \leftrightarrow X^3\Sigma^-$  transition (336 nm,  $1/A = 400$  ns). It has been predicted [1] that  $^3\Sigma$  molecules with relatively large rotational splitting and weak spin-spin interaction (such as the imidogen radical) will be less likely to undergo collision induced Zeeman transitions. Another important feature of the NH system is that imidogen can be produced in a high flux beam with a room temperature discharge source [31]. This provides a new challenge - the introduction of this beam into our very low temperature trapping region. This was a key experimental challenge that was met with success and can be applied to numerous other species.

Our apparatus is centered around a cold cell made from copper [38] and is thermally disconnected from the 4 K magnet surrounding it (see Fig. 1). The maximum trap depth available is 3.9 Tesla. Windows at the magnet midplane allow optical access for laser beams and a fluorescence collection lens. The cell is thermally connected to a  $^3\text{He}$  refrigerator, giving the cell a base temperature of 450 mK.

Buffer gas enters the cell through a fill line and exits out a 3 mm diameter opening in the side of the cell that faces the discharge source (the “molecular beam input aperture” shown in Fig. 1). Helium is continuously supplied to the cell in order to maintain a constant helium atom density in the trapping region.

The constant flow of helium buffer gas out of the cell aperture poses a significant technical problem. The helium gas can scatter imidogen radicals out of the incident NH beam before they enter the trapping cell. In order to maintain sufficient vacuum just outside the cell, a charcoal coated copper tube (“charcoal tube”) is used to pump away the escaping helium. The charcoal tube is held at 4 K so as to act as a low-profile high-speed vacuum pump. This eliminates any significant scattering of imidogen radicals.

The helium buffer gas density in the cell is determined by the rate at which we flow helium into the cell and the conductance out of the molecular beam input aperture. The conductance of the molecular beam input aperture was measured using a fast ion gauge, agreeing with our calculated theoretical value. This system allows both experimental control and absolute knowledge of the buffer-gas density to better than 20%.

The imidogen radicals in the trapping region are detected using laser induced fluorescence (LIF) excited on the  $|A^3\Pi_2, v' = 0, N' = 1\rangle \leftarrow |X^3\Sigma^-, v'' = 0, N'' = 0\rangle$  transition. The light source is a CW dye laser frequency doubled in BBO in an external buildup cavity. The excitation laser beam enters the cell and passes through the trap center along a diameter before exiting. Fluorescence from  $A \rightarrow X$  is collected by a midplane lens perpendicular to both the laser and molecular beam axes and imaged to the face of a photomultiplier tube (PMT). In this way, time-resolved narrow-band spectra of trapped imidogen radicals are gathered. As the spherical quadrupole field of the trap magnet is strongly inhomogeneous and the LIF line frequency is field-dependent, laser frequency maps directly to distance from the trap center.

Figure 2 shows a series of time profiles of the number of trapped imidogen molecules for several different loading times. This signal is simply the PMT count rate versus time using an LIF excitation frequency set to the peak of the trapped imidogen spectral feature. As this is a fluorescence experiment, the absolute number of molecules is difficult to determine accurately. By calculating the efficiency of our detection system, excitation probability, and detected molecule fraction we can, however, put a lower bound on our initial number of trapped imidogen radicals of  $> 10^8$ . The data shown in Fig. 2 was taken with  $^4\text{He}$ , so the

temperature of the buffer-gas cell was elevated to 730 mK (in order to maintain sufficient  $^4\text{He}$  density) at a trap depth of 3.3 Tesla. Each trace corresponds to a different duration of loading from the molecular beam source - the tail ends of all four traces fit well to a single-exponential decay with time constant of  $90 \pm 10$  ms. For loading times less than the molecular trap lifetime, the number of trapped molecules increases nearly in proportion with with loading time (see curves (a), (b) and (c)). This demonstrates one of the key features of the continuous molecular beam loading technique: as the lifetime of molecules in the trap increases, the loading time can be increased resulting in more trapped molecules. Ablation sources for buffer-gas loading experiments have to this point shown insignificant increases in numbers trapped from multiple loading pulses, likely due to the violent nature of the ablation plume in the trapping region. Fig. 2(c,d) shows that as the loading time exceeds the trap lifetime the signal height saturates and there is no longer any significant increase in the number of trapped molecules, as expected.

Trapping is spectroscopically verified by tuning the LIF laser to be resonant with high-field-seeking (HFS) molecules and comparing time profiles to low-field seekers (LFS). The HFS molecules quickly leave the trap and are undetectable after 10 ms while the lifetimes of the LFS molecules are enhanced to more than 200 ms at our lowest loading temperature. The spatial sensitivity of our fluorescence collection precludes fitting the spectra for temperature, but we have previously demonstrated rotational and translational thermalization of imidogen to the buffer gas temperature [31]. Finally, as described below, only trapped molecules produce the lifetimes vs. trap depths that we observe.

In the absence of collisional losses, the trap lifetime will increase significantly as trap depth increases and the magnetic trapping field holds molecules in the center of the cell. With background buffer gas present, there is an additional lifetime lengthening factor as collisions with helium atoms slow motion of trapped molecules to the walls, essentially enforcing diffusive motion. Fig. 3(a) (inset) shows the measured trap lifetime as a function of  $\eta \equiv \mu B_{\text{max}}/k_{\text{B}}T$ , where  $\mu B_{\text{max}}$  is the trap depth. The lifetime is plotted in units of the field-free diffusion lifetime in the cell,  $\tau_o$ , given by [35]

$$\tau_o = \frac{16n\sigma_d}{3\sqrt{2\pi}} \sqrt{\frac{m_{\text{red}}}{k_{\text{B}}T}} \left[ \left(\frac{\alpha_1}{R}\right)^2 + \left(\frac{\pi}{h}\right)^2 \right]^{-1} \quad (1)$$

where  $n$  is the  $^3\text{He}$  buffer-gas density,  $\sigma_d$  is the thermal average of the diffusion cross section,  $R$  and  $h$  are the internal radius and length of the cell,  $m_{\text{red}}$  is the reduced mass of the NH-

$^3\text{He}$  system and  $\alpha_1$  is the first root of the Bessel function  $J_0$  of order zero. For the data in Fig. 3(a) the buffer gas density was  $8.5 \times 10^{14} \text{ cm}^{-3}$  and the temperature was 690 mK. The solid curve is a fit of a numerical solution to the diffusion equation including the trap potential [36] and the only fitting parameter is the cross section, yielding a measurement of  $\sigma_d = 2.7 \pm 0.8 \times 10^{-14} \text{ cm}^2$ . The quoted uncertainty is systematic and dominated by uncertainty in the buffer-gas density. Multiplying this by the average relative velocity of  $\text{NH}-^3\text{He}$  gives the rate coefficient for energy transport,  $k_d = 2.1 \pm 0.6 \times 10^{-10} \text{ cm}^3\text{s}^{-1}$ . This is in good agreement with the 0.5 K energy transport collision rate of  $1.49 \times 10^{-10} \text{ cm}^3\text{s}^{-1}$  calculated by Krems *et al.* in Ref. [1].

Figure 3(b) shows the measured trap lifetime for different buffer-gas densities. The peak lifetime in this study is somewhat low since cell was heated to 710 mK in order to maintain a constant temperature throughout the full buffer-gas density range (a technical artifact of the helium gas supply system). Trapped imidogen lifetimes for the *base* temperature of the cell exceed 200 ms. As the density of the  $^3\text{He}$  buffer gas is increased from  $10^{14}$  to around  $10^{15} \text{ cm}^{-3}$  the lifetime of the trapped molecules increases due to the diffusion effect mentioned above. However, as the  $^3\text{He}$  density is increased past  $10^{15} \text{ cm}^{-3}$  it is seen that the lifetime decreases. This decrease is due to collision-induced Zeeman relaxation of the imidogen radicals as they collide with  $^3\text{He}$ . The time profiles still show good single-exponential decay behavior for these higher buffer-gas densities.

To extract a rate constant for these inelastic collisions, we fit a model curve to the data in Fig. 3. After being loaded, the time profile of the molecule number in the trap can be modeled as  $N(t) = N_o e^{-tA/n} e^{-tnk_{\text{in}}}$  where  $n$  is the buffer gas density,  $N_o$  is the initial number of imidogen radicals after loading, and  $A$  and  $k_{\text{in}}$  are fitting parameters corresponding to diffusion enhancement of the lifetime and inelastic collision loss, respectively. This can be rewritten as a single exponential with a time constant given by  $1/\tau_{\text{eff}} = A/n + nk_{\text{in}}$ , which gives the form for the curve fitted to the data in Fig. 3. The constant  $k_{\text{in}}$  is the collision induced Zeeman relaxation rate at 710 mK and is found to be  $k_{\text{in}} = 3.0 \pm 0.9 \times 10^{-15} \text{ cm}^3\text{s}^{-1}$ , corresponding to an inelastic cross section of  $\sigma_{\text{in}} = 3.8 \pm 1.1 \times 10^{-19} \text{ cm}^2$  and therefore a ratio of diffusive to inelastic cross sections of  $\gamma = 7 \times 10^4$ . The uncertainties are systematic and are dominated by uncertainty in the absolute buffer-gas density. This inelastic collision rate is an order of magnitude higher than the 500 mK value of  $4.20 \times 10^{-16} \text{ cm}^3\text{s}^{-1}$  for 100 Gauss given by Krems *et al.* [1] and may be larger due to the strong temperature dependence of the

predicted shape resonance. Furthermore, the rate we measure is averaged over the magnetic field range of our trap, and inelastic collision cross sections are predicted to become strongly field-dependent just below this collision energy [1, 29].

In summary, we have demonstrated magnetic trapping of ground state imidogen molecules using buffer gas loading from a molecular beam. The energy transport (diffusion) and inelastic collision rate constants for  $\text{NH-}^3\text{He}$  have been measured

resulting in a ratio of elastic to inelastic collision rates of  $7 \times 10^4$ , which indicates that imidogen radicals should be amenable to the pumping out of the buffer gas and thermal isolation. It is particularly interesting to note that we are able to trap imidogen near the peak of the narrow shape resonance predicted by Krems *et al.* in Ref. [1]. A factor of two decrease (or increase) in collision energy would decrease the inelastic rate by more than a factor of ten, resulting in a increase in  $\gamma$  to nearly  $10^6$ . This bodes very well for both increasing the number of trapped molecules and perhaps for sympathetic cooling of large numbers of imidogen radicals and other hydrides to the ultracold regime.

We thank Katsunari Enomoto and Michael Gottselig for their valuable assistance in the design and fabrication of the apparatus and also greatly acknowledge Colin Connolly for his construction of the  $^3\text{He}$  refrigerator used in these experiments. The authors are grateful to B. Friedrich and R. Krems for discussions and careful reading of the manuscript and G. C. Groenenboom for helpful discussions. This work was supported by the U.S. Department of Energy under Contract No. DE-FG02-02ER15316 and the U.S. Army Research Office.

---

\* wes@cua.harvard.edu

† Current address: Max-Planck-Institut für Quantenoptik, Garching, Germany

- [1] R. V. Krems, H. R. Sadeghpour, A. Dalgarno, D. Zgid, J. Kłos, and G. Chałasiński, *Phys. Rev. A* **68**, 051401(R) (2003).
- [2] J. Doyle, B. Friedrich, R. V. Krems, and F. Masnou-Seeuws, *Eur. Phys. J. D* **31**, 149 (2004).
- [3] H. L. Bethlem and G. Meijer, *Int. Rev. Phys. Chem.* **22**, 73 (2003).
- [4] D. DeMille, *Phys. Rev. Lett.* **88**, 067901 (2002).
- [5] A. André, D. DeMille, J. M. Doyle, M. D. Lukin, S. E. Maxwell, P. Rabl, R. J. Schoelkopf, and P. Zoller, *Nature Physics* **2**, 636 (2006).

- [6] A. Micheli, G. K. Brennen, and P. Zoller, *Nature Physics* **2**, 341 (2006).
- [7] M. G. Kozlov and L. N. Labzowsky, *J. Phys. B: At. Mol. Opt. Phys.* **28**, 1933 (1995).
- [8] S. Schiller and V. Korobov, *Phys. Rev. A* **71**, 032505 (2005).
- [9] N. Balakrishnan and A. Dalgarno, *Chem. Phys. Lett.* **341**, 652 (2001).
- [10] R. V. Krems, *Int. Rev. Phys. Chem.* **24**, 99 (2005).
- [11] J. L. Bohn, A. V. Avdeenkov, and M. P. Deskevich, *Phys. Rev. Lett.* **89**, 203202 (2002).
- [12] A. V. Avdeenkov, M. Kajita, and J. L. Bohn, *Phys. Rev. A* **73**, 022707 (2006).
- [13] G. S. F. Dhont, J. H. van Lenthe, G. C. Groenenboom, and A. van der Avoird, *J. Chem. Phys.* **123**, 184302 (2005).
- [14] M. Kajita, *Phys. Rev. A* **74**, 032710 (2006).
- [15] M. Lara, J. L. Bohn, D. Potter, P. Soldán, and J. M. Hutson, *Phys. Rev. Lett.* **97**, 183201 (2006).
- [16] J. M. Sage, S. Sainis, T. Bergeman, and D. DeMille, *Phys. Rev. Lett.* **94**, 203001 (2005).
- [17] E. A. Donley, N. R. Claussen, S. T. Thompson, and C. E. Wieman, *Nature* **417**, 529 (2002).
- [18] H. L. Bethlem, G. Berden, and G. Meijer, *Phys. Rev. Lett.* **83**, 1558 (1999).
- [19] R. Fulton, A. I. Bishop, M. N. Schneider, and P. F. Barker, *J. Phys. B: At. Mol. Opt. Phys.* **39**, S1097 (2006).
- [20] M. S. Elioff, J. J. Valentini, and D. W. Chandler, *Science* **302**, 1940 (2003).
- [21] J. D. Weinstein, R. deCarvalho, T. Guillet, B. Friedrich, and J. M. Doyle, *Nature* **395**, 148 (1998).
- [22] J. M. Bakker, M. Stoll, D. R. Weise, O. Vogelsang, G. Meijer, and A. Peters, *J. Phys. B* **39**, S1111 (2006).
- [23] R. deCarvalho, N. Brahm, B. Newman, J. M. Doyle, D. Kleppner, and T. Greytak, *Can. J. Phys.* **83**, 293 (2005).
- [24] D. M. Silveira, O. Pereira, M. Veloso, and C. L. Cesar, *Brazilian Journal of Physics* **31**, 203 (2001).
- [25] J. D. Weinstein, R. deCarvalho, K. Amar, A. Boca, B. C. Odom, B. Friedrich, and J. M. Doyle, *J. Chem. Phys.* **109**, 2656 (1998).
- [26] K. Maussang, D. Egorov, J. S. Helton, S. V. Nguyen, and J. M. Doyle, *Phys. Rev. Lett.* **94**, 123002 (2005).
- [27] M. Stoll, private communication.



- [28] R. V. Krems and A. Dalgarno, *J. Chem. Phys.* **120**, 2296 (2004).
- [29] H. Cybulski, R. V. Krems, H. R. Sadeghpour, A. Dalgarno, J. Kłos, G. C. Groenenboom, A. van der Avoird, D. Zgid, and G. Chałasiński, *J. Chem. Phys.* **2005**, 094307 (2005).
- [30] S. Y. T. van de Meerakker, I. Labazan, S. Hoekstra, J. Küpper, and G. Meijer, *J. Phys. B: At. Mol. Opt. Phys.* **39**, S1077 (2006).
- [31] D. Egorov, W. C. Campbell, B. Friedrich, S. E. Maxwell, E. Tsikata, L. D. van Buuren, and J. M. Doyle, *Eur. Phys. J. D* **31**, 307 (2004).
- [32] H. Lewandowski, L. P. Parazzoli, D. Lobser, and C. Romero, in *379. WE-Heraeus-Seminar on Cold Molecules* (2006).
- [33] S. Y. T. van de Meerakker, B. G. Sartakov, A. P. Mosk, R. T. Jongma, and G. Meijer, *Phys. Rev. A* **68**, 032508 (2003).
- [34] W. Ubachs, J. J. ter Meulen, and A. Dymanus, *Can. J. Phys.* **62**, 1374 (1984).
- [35] J. B. Hasted, *Physics of Atomic Collisions* (American Elsevier Publishing Company, Inc., 1972), chap. 1.6, 2nd ed.
- [36] J. D. Weinstein, Ph.D. thesis, Harvard University (2001).
- [37] J. G. E. Harris, R. A. Michniak, S. V. Nguyen, W. C. Campbell, D. Egorov, S. E. Maxwell, L. D. van Buuren, and J. M. Doyle, *Rev. Sci. Inst.* **75**, 17 (2004).
- [38] Alloy C10100, annealed in forming gas.

## Figures

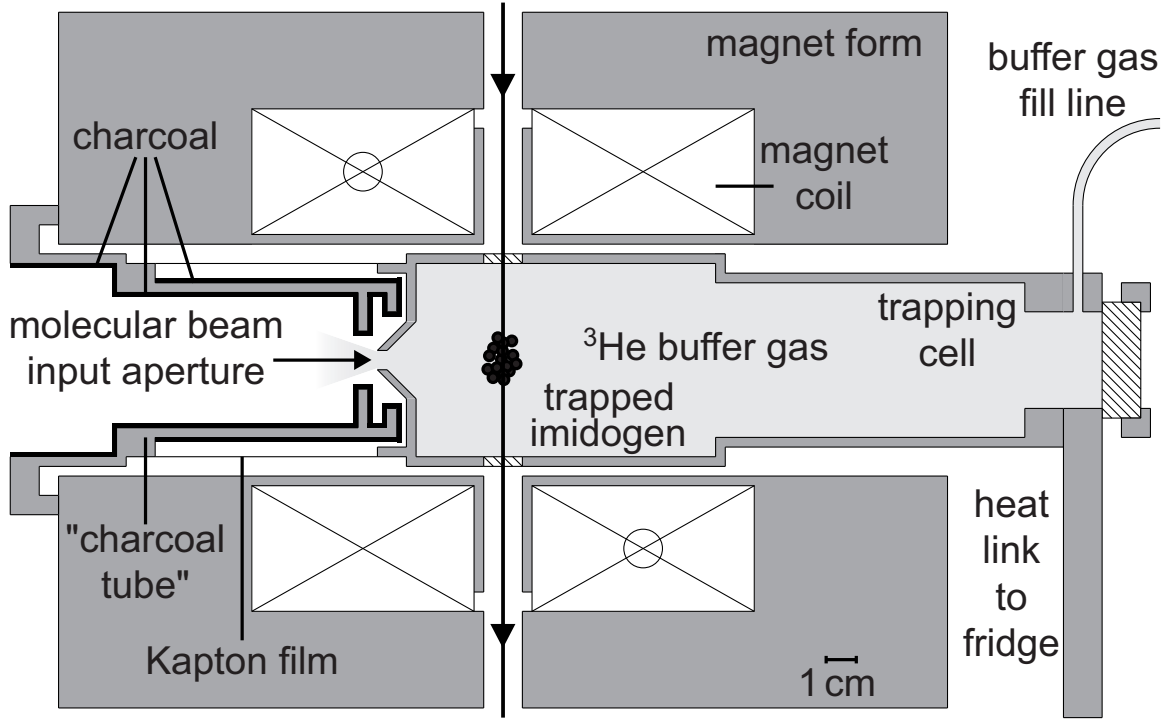


FIG. 1: Schematic diagram of the magnetic trap, buffer-gas cell and charcoal tube in vacuum. The imidogen beam is produced by flowing ammonia from a pulsed valve through a slit glow discharge 12 cm to the left of the molecular beam input aperture. The radical beam propagates through openings in the 77 K and 4 K blackbody radiation shields (not shown), through a section of the magnet bore, through the molecular beam input aperture and into the trapping cell. The trap magnet surrounds the trapping cell and is described in Ref. [37].

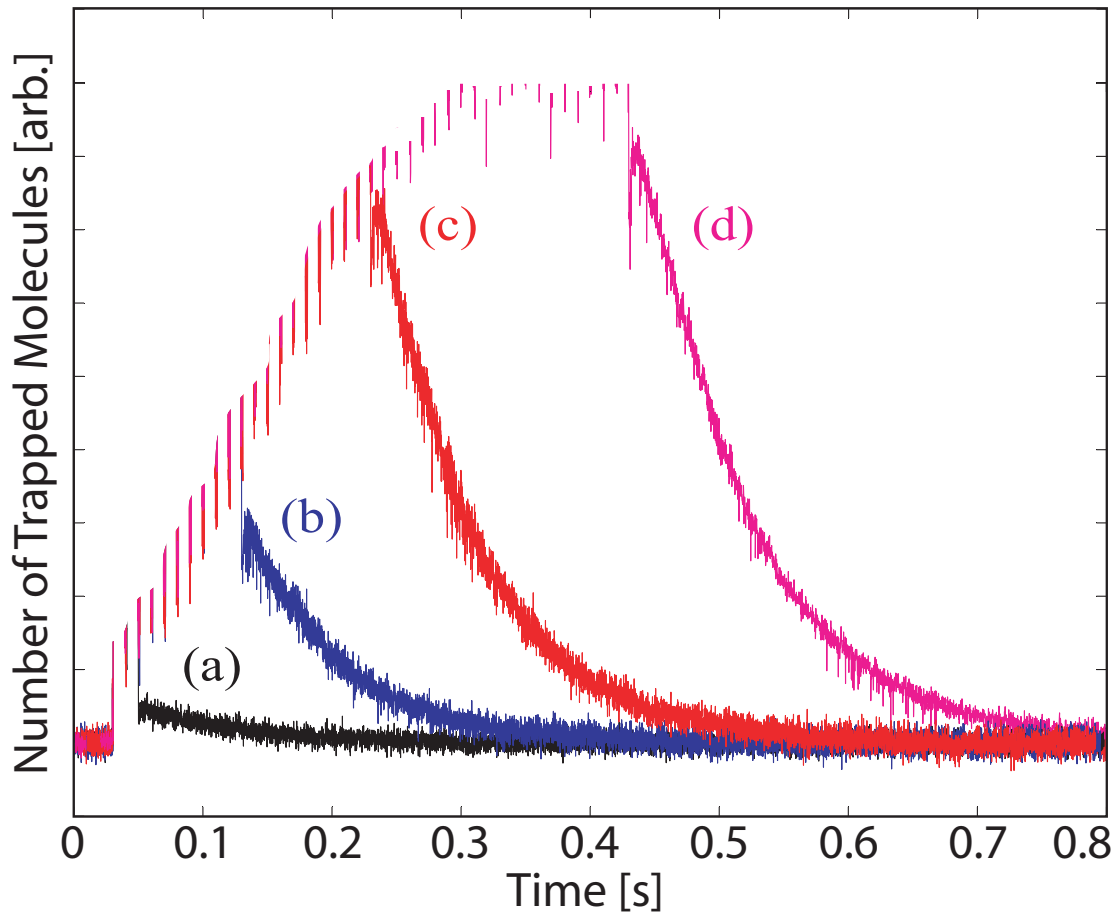


FIG. 2: Time profiles of the fluorescence signal gathered by the PMT. The curves correspond to different durations of the molecular beam loading pulse of (a) 10 ms, (b) 100 ms, (c) 200 ms and (d) 400 ms. The dissociation discharge causes periodic overranging of the signal during loading.

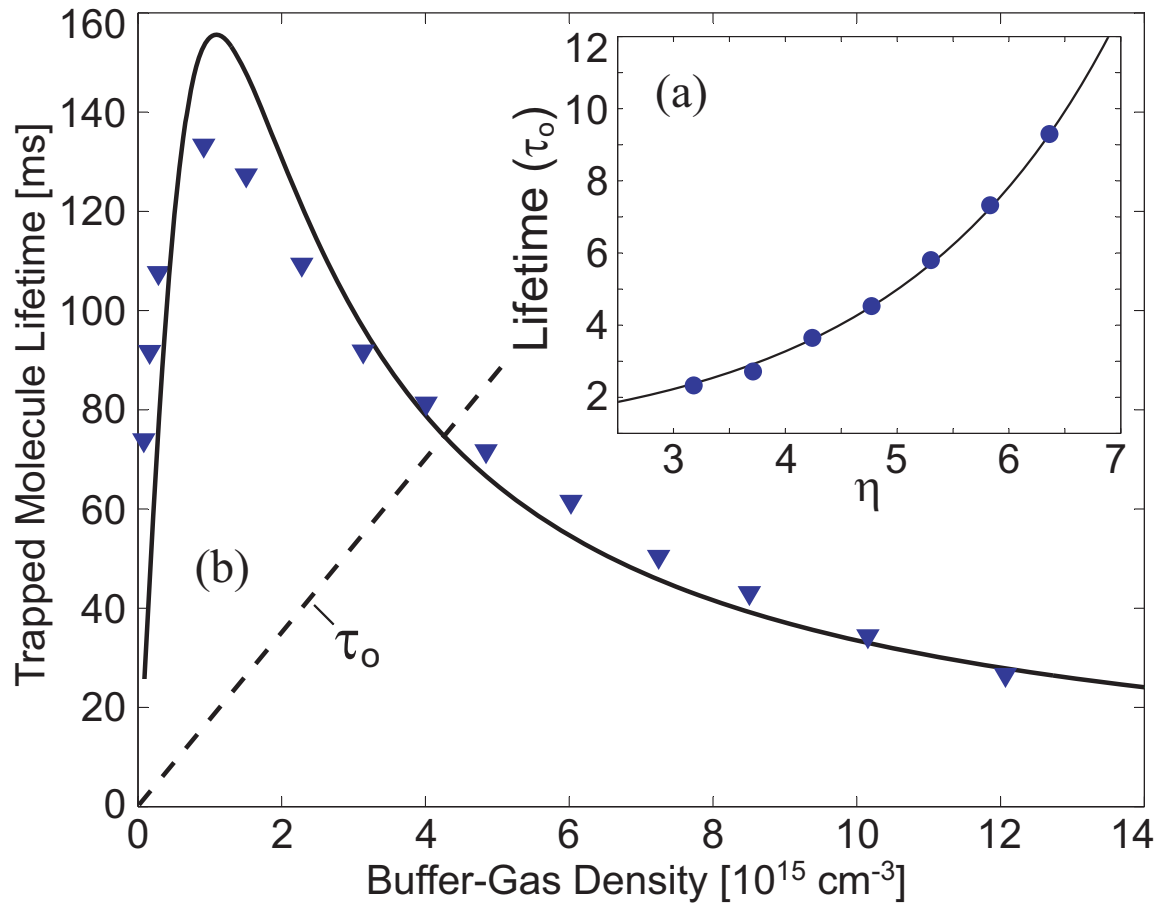


FIG. 3: Lifetimes for magnetically trapped imidogen radicals vs. (a) trap depth and (b) buffer-gas density. Trapped molecule lifetimes were obtained by fitting the fluorescence to a single-exponential decay.  $\tau_0$  is the field-free diffusion lifetime calculated from Eq. 1. The solid curve in (b) is a two-parameter fit of the form  $1/\tau_{\text{eff}} = A/n + nk_{\text{in}}$  and yields the inelastic cross section.